Electrochemical and Solid-State Letters, **11** (1) H7-H9 (2008)
1099-0062/2007/11(1)/H7/3/$23.00 © The Electrochemical Society

Solution-Processed Indium-Zinc Oxide Transparent Thin-Film Transistors

Chaun Gi Choi, Seok-Jun Seo, and Byeong-Soo Bae[z]

Laboratory of Optical Materials and Coating, Department of Materials Science and Engineering, Korea Advanced Institute of Science and Technology, Daejeon 305-701, Korea

Transparent thin-film transistors (TTFTs) with an indium-zinc oxide (IZO) active layer by the solution-processed deposition method were fabricated and their TFT characterization was examined. Solution-processed IZO thin films were amorphous and highly transparent with >90% transmittance in the visible region with an optical bandgap of 3.1 eV. Spin-coated IZO TTFTs were operated in depletion mode and showed a field-effect mobility as high as 7.3 cm^2/V s, a threshold voltage of 2.5 V, an on/off current ratio greater than 10^7, and a subthreshold slope of 1.47 V/decade.
© 2007 The Electrochemical Society. [DOI: 10.1149/1.2800562] All rights reserved.

Manuscript submitted August 20, 2007; revised manuscript received September 21, 2007.
Available electronically October 29, 2007.

Metal-oxide thin films have been traditionally used as insulators, dielectrics, and conductors in (opto)electronic devices. Recently, metal-oxide thin films have been intensively studied to be applied as transparent semiconducting active layers in transparent thin-film transistors (TTFTs). Transparent oxide semiconductors (TOSs) have many advantages compared to silicon or organic semiconductors. TOSs are transparent in the visible region due to their large bandgap and have environmental stability and high field-effect mobility comparable to that of polycrystalline silicon.[1,2] Many TOSs such as ZnO,[3,4] zinc-tin oxide (ZTO),[5,6] indium-zinc oxide (IZO),[7-9] and indium-gallium-zinc oxide (IGZO)[2,10,11] have been reported for transparent active-channel materials in TTFTs. Several TTFTs using TOSs[12,13] and even fully transparent flexible structures[3,14] have been reported. TTFTs based on TOSs are considered to be an alternative to amorphous Si TFTs. However, TOSs are generally prepared by vacuum-deposition methods such as rf magnetron sputtering and pulsed laser deposition. Vacuum-deposition methods require expensive equipment and result in high manufacturing costs.

Solution-processed thin-film deposition methods could offer many advantages such as simplicity, low cost, and high throughput that enable the fabrication of high-performance and low-cost electronics. In addition, solution-processed deposition methods such as screen printing, inkjet printing, and imprinting offer the possibility of the direct patternability of TOS thin films which could replace the conventional photolithographic technique. Recently, ZnO,[15-17] ZTO,[18] and IZO-based[19] TTFTs fabricated by solution-processed deposition using metallorganic or metal halide precursors in various solvents were reported to have high mobility up to ~16 cm^2/V s and to give direct patternability. However, in the case of using metal chloride as precursors, the presence of chloride ions during heat-treatment of the film is unfavorable under certain circumstances. In addition, TTFTs fabricated by solution-processed deposition showed high off currents and a low on/off current ratio compared to the vacuum-deposited TTFTs.

In this article, we report the amorphous IZO semiconductor thin films fabricated by solution process under ambient air conditions using metal acetates as precursors and the performance of TTFTs with an amorphous IZO active layer. Spin-coated IZO thin film was uniform, highly transparent in the visible spectrum region, and stable in air conditions. The TTFTs with amorphous IZO semiconductor with an inverted-gate structure were demonstrated comparable TFT performance to those using vacuum-deposited TOSs.

Experimental

Precursor solution for fabricating IZO thin films was prepared by dissolving 0.1 M of zinc acetate dihydrate [$Zn(OAc)_2 \cdot 2H_2O$] and 0.1 M of indium acetate [$In(OAc)_3$] in 2-methoxyethanol at 50°C. $Zn(OAc)_2 \cdot 2H_2O$ has limited solubility in alcohols and its precursor solution is easily precipitated or gelled. $In(OAc)_3$ is not soluble in 2-methoxyethanol. Thus, $Zn(OAc)_2 \cdot 2H_2O$ and $In(OAc)_3$ require stabilizing agents for dissolution and formation of stable sol.[20-23] Diethanolamine (DEA) of 0.4 M and acetylacetone (acac) of 0.4 M were used to stabilize the IZO precursor solution.

Heavily boron (p^+)-doped silicon substrate was used in an inverted-gate structure for the fabrication of IZO-based TTFTs. Silicon dioxide with a thickness of 120 nm was thermally grown on top of the silicon substrate and used as gate dielectric. IZO solution was spin-coated on the SiO_2/Si substrates at a speed of 8000 rpm for 30 s and annealed at 500°C for 1 h in a furnace in an atmospheric environment. An IZO thin film with a thickness of about 10 nm was obtained on top of the SiO_2. Aluminum, which was used as source and drain electrodes, was then evaporated on top of the IZO semiconductor layer through a shadow mask with a channel width of 1000 μm and a channel length of 120 μm to complete the fabrication process of IZO-based TTFTs. Device characterization was performed in the dark at room temperature using two Keithley 236 source-measure units.

Results and Discussion

To determine the heat-treatment temperature, thermogravimetric analysis (TGA) was performed under air atmosphere at a heating rate of 5°C/min using a TGA Q50 analyzer (TA instruments). Figure 1 shows the TGA curve of the IZO precursor solution dried at 150°C to remove the solvent and the water and ground into powder. The initial weight loss to 190°C represents the evaporation of ab-

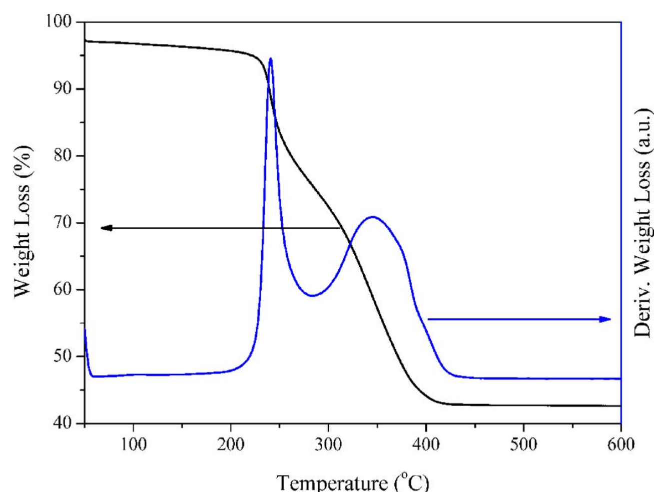

Figure 1. (Color online) TGA of IZO precursor solution at 5°C/min heating rate.

[z] E-mail: bsbae@kaist.ac.kr

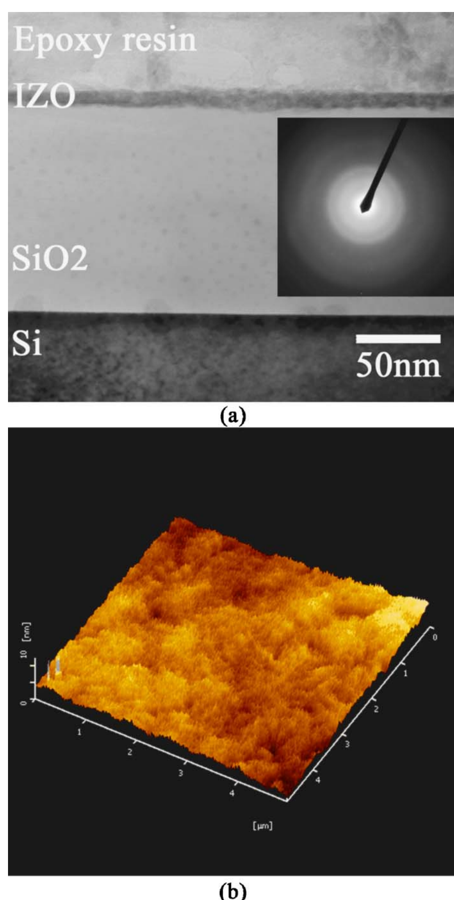

Figure 2. (Color online) (a) Cross-sectional TEM image and electron diffraction pattern (inset) and (b) AFM image of the spin-coated IZO thin film on the SiO_2/Si substrate.

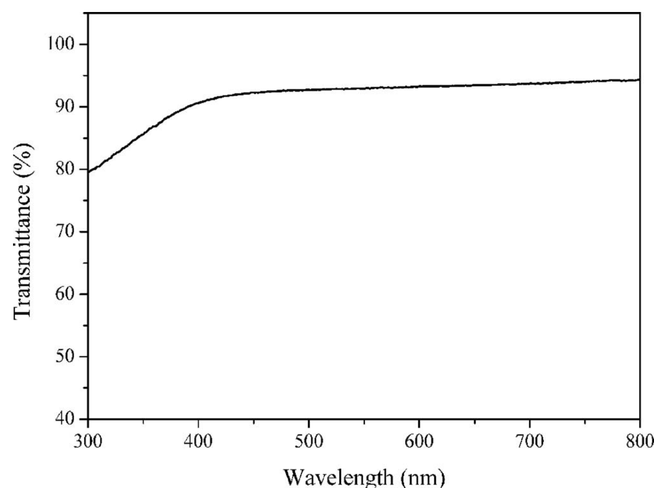

Figure 3. UV/vis transmittance spectrum of spin-coated ZTO thin films on a quartz substrate.

sorbed moisture and the residual solvents, including 2-methoxyethanol. The TGA curve shows that IZO precursor solution loses weight through two steps and its derivative maxima are at ~240 and ~350°C. The weight loss at ~240 and ~350°C represents the decomposition of $Zn(OAc)_2$[15] and $In(OAc)_3$,[21] respectively. The weight-loss tail at 400°C might come from the decomposition of the residual amorphous material, which is related to oxidative removal of residual organics.[23] Beyond 500°C, no detectable weight loss was observed. This result suggests the heat-treatment temperature of 500°C would be sufficient to remove all the organics for the formation of amorphous IZO thin film.

IZO thin-film thickness was measured by transmission electron microscopy (TEM) (JEM 3010, JEOL) with an acceleration voltage of 200 kV. The surface morphology of IZO thin films was observed by atomic force microscopy (AFM) (SPI 3800N, SEIKO). Figure 2a shows the cross-sectional TEM image of the IZO thin film on SiO_2/Si substrate with a thickness of about 10 nm. The inset of Fig. 2a shows diffraction patterns of IZO thin film which did not show any characteristic patterns, which means that the spin-coated IZO thin film is amorphous. An AFM image, as shown in Fig. 2b, reveals that the IZO thin film has a smooth and homogeneous surface with a low root-mean-square (rms) roughness of ~1 nm and shows no crystalline grains.

The optical transmission analysis of the IZO thin films was carried out at various wavelengths using ultraviolet-visible-near infrared (UV/vis/NIR) spectroscopy (UV3101PC, Shimadzu). Figure 3 shows the optical transmission spectrum of the amorphous IZO thin film deposited on the quartz substrate in the wavelength range from 300 to 800 nm. The spectrum shows that IZO thin film is highly transparent with >90% transmittance in the visible spectrum region (400–700 nm). The optical absorption coefficient (α) calculated from the transmittance was used to determine the optical bandgap (E_g) and is given by the relation

$$(\alpha h\nu)^2 = (h\nu - E_g) \qquad [1]$$

where $h\nu$ is the photon energy. The optical bandgap can be determined by the extrapolation of the linear region from a plot of α^2 vs photon energy ($h\nu$) near the onset of the absorption edge to the photon energy axis. The optical bandgap of the IZO thin film was measured to be 3.1 eV, which is similar to the value reported for other IZO thin films.[19,24]

Figure 4a shows the output curves of the TTFT with a 10 nm thick IZO active layer at various gate voltages. The IZO TTFT behaves as a n-channel transistor and exhibits good linear/saturation behavior. Figure 4b shows the transfer curve of the IZO TTFT with a drain-source voltage (V_{DS}) of 40 V. At zero gate voltage (V_G = 0 V), there is considerable drain current and the channel is not pinched off completely until the application of negative gate voltages. Because the IZO semiconductors are n-type channels, this behavior indicates that the device is operating in depletion mode. This means that there are many mobile charge carriers in the IZO thin films. It is known that the primary carrier sources come from the native defect doping by doubly charged oxygen vacancies which are donating the electrons in the IZO.[7] The electrical parameters were determined from a plot of $I_D^{1/2}$ vs V_G on the basis of the following relationship in the saturation regime

$$I_D = \frac{WC_i}{2L}\mu(V_G - V_{th})^2 \qquad [2]$$

where I_D is the drain current, W and L are the channel width and length, respectively, μ is the field-effect mobility, C_i is the capacitance per unit area, and V_{th} is the threshold voltage. The IZO TTFT has a field-effect mobility of 7.3 cm^2/V s and a threshold voltage of 2.5 V. We designated the exponentially increasing onset position to on-current state as turn-on voltage ($V_{turn-on}$). The $V_{turn-on}$ of the solution-processed IZO TTFTs is around −20 V. The mobility of the spin-coated IZO TTFT is relatively lower than that fabricated by vacuum deposition. However, because the mobility of 1–10 cm^2/V s seems to be sufficient to meet the brightness and resolution requirements for active matrix organic light-emitting diodes (AMOLEDs),[25] the spin-coated IZO TTFTs can be applicable to the backplane of the AMOLED.

The important transistor parameters for use in active-matrix TFT applications are the device on/off current ratio and subthreshold

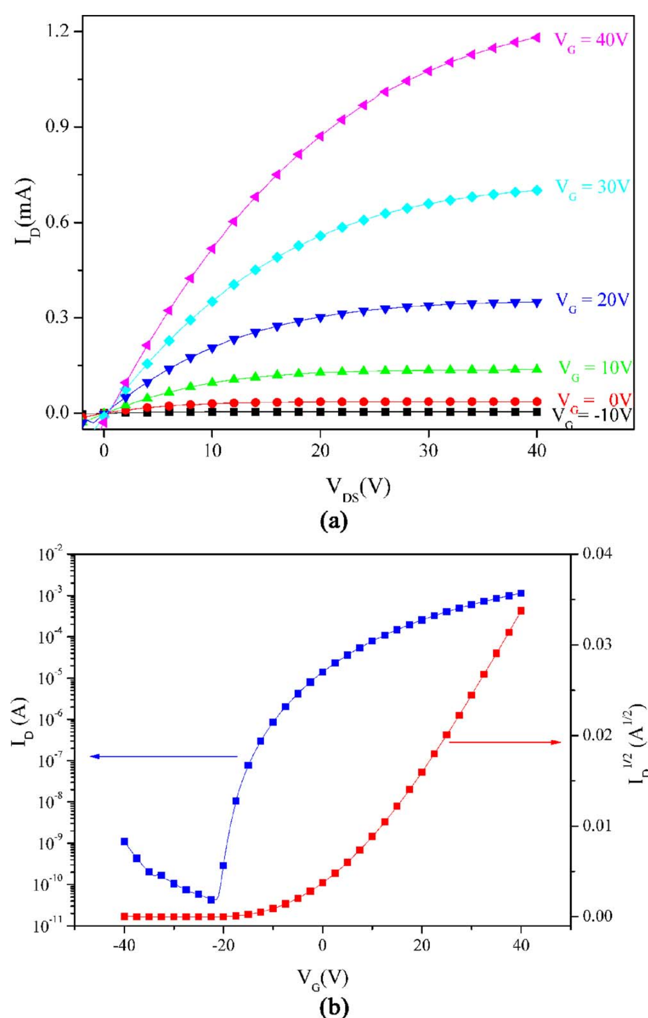

Figure 4. (Color online) (a) Output characteristics and (b) transfer characteristics of the spin-coated IZO TFT with V_{DS} at 40 V.

slope. The off current of the IZO TTFT is low, on the order of 4.2×10^{-11} A at $V_{turn\text{-}on}$, which is quite small in comparison to those of the solution-processed TTFTs.[15-19] The low off current is attributed to the fact that the IZO thin film is thin, amorphous, and free of mobile ions which prevent the charge carriers from conducting through the bulk of the IZO semiconductor. The on/off current ratio is greater than 10^7, which indicates that the IZO TTFT is applicable to the switching devices in active-matrix flat-panel displays. The subthreshold slope, S, defined as the voltage required to increase the drain current by a factor of 10, was 1.47 V/decade. In this work, the S of the IZO TTFTs is lower that those of other solution-processed IZO TTFTs[19] and is compatible with those of the vacuum-deposited IZO TTFTs.[7,26] However, the S of spin-coated IZO TTFT is larger than other vacuum-deposited TTFTs.[27] As the S is correlated with the doping density in IZO semiconductor,[28] the relatively high S is attributed to many electrons in the IZO thin films, which may come from the doubly charged oxygen vacancies.[7]

Conclusion

We synthesized the precursor solution for the deposition of IZO thin film. Highly transparent and amorphous IZO thin films were obtained by annealing at 500°C using this precursor solution. A depletion-mode TTFT was fabricated using the spin-coated IZO channel layer. The IZO TTFT has a field-effect mobility of 7.3 cm^2/V s, a threshold voltage of 2.5 V, a subthreshold slope of 1.47 V/dec., and a current on-to-off ratio greater than 10^7, respectively. The solution-processed TOSs could provide the possibility of producing high-performance TTFTs for simple and low-cost large-area electronics.

The Korea Advanced Institute of Science and Technology assisted in meeting the publication costs of this article.

References

1. J. F. Wager, *Science*, **300**, 1245 (2003).
2. K. Nomura, H. Ohta, K. Ueda, T. Kamiya, M. Hirano, and H. Hosono, *Science*, **300**, 1269 (2003).
3. E. M. C. Frotunato, P. M. C. Barquinha, A. C. M. B. G. Pimentel, A. M. F. Goncalves, A. J. S. Marques, L. M. N. Pereira, and R. F. P. Martins, *Adv. Mater. (Weinheim, Ger.)*, **17**, 590 (2005).
4. R. L. Hoffman, B. J. Norris, and J. F. Wager, *Appl. Phys. Lett.*, **82**, 733 (2003).
5. H. Q. Chiang, J. F. Wager, R. L. Hoffman, J. Jeong, and D. A. Keszler, *Appl. Phys. Lett.*, **86**, 013503 (2005).
6. W. B. Jackson, R. L. Hoffman, and G. S. Herman, *Appl. Phys. Lett.*, **87**, 193503 (2005).
7. B. Yaglioglu, H. Y. Yeom, R. Beresford, and D. C. Paine, *Appl. Phys. Lett.*, **89**, 062103 (2006).
8. P. Barquinha, A. Pimentel, A. Marques, L. Pereira, R. Martins, and E. Fortunato, *J. Non-Cryst. Solids*, **352**, 1749 (2006).
9. N. L. Dehuff, E. S. Kettenring, D. Hong, H. Q. Chiang, J. F. Wager, R. L. Hoffman, C.-H. Park, and D. A. Keszler, *J. Appl. Phys.*, **97**, 064505 (2005).
10. K. Nomura, T. Kamiya, H. Ohta, K. Ueda, M. Hirano, and H. Hosono, *Appl. Phys. Lett.*, **85**, 1993 (2004).
11. A. Suresh, P. Wellenius, A. Dhawan, and J. Muth, *Appl. Phys. Lett.*, **90**, 123512 (2007).
12. T. Kamiya, H. Hiramatsu, K. Nomura, and H. Hosono, *J. Electroceram.*, **17**, 267 (2006).
13. T. Kamiya, S. Narushima, H. Mizoguchi, K. Shimizu, K. Ueda, M. Hirano, and H. Hosono, *Adv. Funct. Mater.*, **15**, 968 (2005).
14. K. Nomura, H. Ohta, A. T. T. Kamiya, M. Hirano, and H. Hosono, *Nature (London)*, **432**, 488 (2004).
15. B. S. Ong, C. Li, Y. Li, Y. Wu, and R. Loutfy, *J. Am. Chem. Soc.*, **129**, 2750 (2007).
16. H.-C. Cheng, C.-F. Chen, and C.-Y. Tsay, *Appl. Phys. Lett.*, **90**, 012113 (2007).
17. B. J. Norris, J. Anderson, J. F. Wager, and D. A. Keszler, *J. Phys. D*, **36**, L105 (2003).
18. Y.-J. Chang, D.-H. Lee, G. S. Herman, and C.-H. Chang, *Electrochem. Solid-State Lett.*, **10**, H135 (2007).
19. D.-H. Lee, Y.-J. Chang, G. S. Herman, and C.-H. Chang, *Adv. Mater. (Weinheim, Ger.)*, **19**, 843 (2007).
20. S. Chakrabarti, D. Ganguli, and S. Chaudhuri, *Mater. Lett.*, **58**, 3952 (2004).
21. R. B. H. Tahar, T. Ban, Y. Ohya, and Y. Takahashi, *J. Appl. Phys.*, **82**, 865 (1997).
22. T. Kawahara, T. Ishida, H. Tada, N. Noma, N. Tohge, and S. Ito, *J. Mater. Sci.*, **38**, 1703 (2003).
23. M. L. Mottern, F. Tyholdt, A. Ulyashin, A. T. J. van Helvoort, H. Verweij, and R. Bredesen, *Thin Solid Films*, **515**, 3918 (2007).
24. K. Ramamoorthy, K. Kumar, R. Chandramohan, K. Sankaranarayanan, R. Saravanan, I. V. Kityk, and P. Ramasamy, *Opt. Commun.*, **262**, 91 (2006).
25. A. Kumar, A. Nathan, and G. E. Jabbour, *IEEE Trans. Electron Devices*, **52**, 2386 (2005).
26. J.-I. Song, J.-S. Park, H. Kim, Y.-W. Heo, J.-H. Lee, J.-J. Kim, G. M. Kim, and B. D. Choi, *Appl. Phys. Lett.*, **90**, 022106 (2007).
27. A. Suresh, P. Wellenius, A. Dhawan, and J. Muth, *Appl. Phys. Lett.*, **90**, 123512 (2007).
28. D. K. Schroder, *Semiconductor Material and Device Characterization*, 3rd ed., Wiley, New York (2006).